Materials and Methods

Animals

Adult, male C57BL/6J mice were obtained from Janvier Labs (Le Genest-Saint-Isle, France), and housed in groups of 5 in individually ventilated cages (IVC, Greenline, Techniplast, Italy) under standard laboratory conditions (22 ± 1 °C, 45-65% humidity, and 12: 12 h light/dark cycle, lights on at 07:00). Food and water was provided *ad libitum*. The behavioural tests were carried out during the light phase of the cycle (between 08:00 a.m. and 3:00 p.m.). Exact n numbers for each experiment are given in the corresponding figure legends. All experiments were carried out in compliance with national and international guidelines for animal welfare as approved by the Austrian Bundesministerium für Bildung, Wissenschaft und Forschung. At the day of theexperiment mice were 11-14 weeks old.

CO_2 Challenge paradigm

CO_2 challenge experiments were conducted in custom-built transparent plexiglass chamber consisting of two vertically stacked chambers (25 x 25 x 25 cm each) separated by a manually rotatable plexiglass partition adapted from a previously described setup[2]. Gas was delivered to the upper compartment through silicone tubing connected to compressed gas cylinders (Messer Austria GmbH, Gumpoldskirchen, Austria). Synthetic air (<0.1% CO_2, 21% O_2, 79% N_2) or pre-mixed gas mixtures containing nominally 10% or 20% CO_2 (counterbalanced with N_2) according to the manufacturer's specifications, were delivered at a flow rate of 9L/min. CO_2 concentrations inside the bottom chamber were continuously monitored using a gas analyzer (GasLab pro, CM-1000 series; CO2Meter Inc., Ormond Beach, FL, USA) placed outside of the chamber via a tube reaching into the chamber. In parallel, room CO_2 levels were measured using an Air CO_2ntrol 5000 device (Dostmann electronic GmbH, Wertheim-Reicholzheim,

Germany) for safety reasons. Illumination at the bottom of the testing arenas was set to approximately 50 lux. A video camera (GoPro HERO, Inc., San Mateo, CA, USA), was mounted in the middle of the dividing partition.

Mice were handled by the experimenter for two consecutive days before the start of the experiment. On experimental day 1, mice were placed into the bottom chamber and allowed to freely explore it for 10 min. On experimental day 2, mice were placed in the chamber, and synthetic air was delivered at a rate of 9 L/min for 10min to habituate the animals to the approximately 65 dB background noise generated by gas flow into the upper chamber. On experimental day 3, mice were randomly divided into three groups. The arena was prefilled with synthetic air, air enriched with 10% CO_2, or air enriched with 20% CO_2, and the partition was closed. Mice were placed into the testing arena and the partition was opened to allow the gas falling gently into the testing chamber. In parallel, gas was delivered at a flow rate of 9 L/min for 5 min to reach the target CO_2 concentration, followed by an additional 5 min period without gas flow, during which CO_2 concentrations remained at the target level. Behaviour was video-recorded. After the experiment, the mice were returned to their home cages

Corticosterone measures

After the 10-min exposure to the chamber, air, 10%CO_2 or 20%CO_2, mice were returned to their home cages. Twenty minutes later they were rapidly decapitated and trunk blood was collected in EDTA-coated blood collection tubes (Minicollect, Greiner Bio-One, Kremsmünster, Austria). To obtain blood plasma, the samples were then centrifuged at 3000 rpm for 10 min. The supernatant was transferred to a fresh sample tube and stored at -20°C for later analysis. Plasma corticosterone levels were measured using a ready-to-use ELISA kit (EIA-4164, DRG Instruments GmbH, Marburg, Germany)[3] according to the manufacturer's instructions (detailed manufacturer's instruction protocol available online). Concentrations results were

indirectly calculated from absorbance readings obtained at 450nm exposure employing an absorbance reader (VICTOR3 TM Multilabel Plate Reader 1420, Perkin Elmer precisely, Finland; Software: PerkinElmer 1420 D manager, and Wallac 1420 Wizard). Samples were diluted to an optimal 1:10 ratio in PBS (1X, pH 7.4), based on a trial conducted beforehand. A calibration curve was generated using standard solutions (in duplicate), and absorbance values from plasma samples were plotted against this curve to extrapolate corticosterone concentrations. Absorbance values were normalized using blank absorbance readings (PBS only samples) and lastly adjusted for the dilution factor. Notably, wavelength correction was not applied to the absorbance values.

Pupillometry

Surgery

All surgeries were performed under isoflurane anesthesia delivered at a constant rate (induction 8%, maintenance 1.5-2.5% isoflurane, Univentor 410 Anesthesia Unit, AgnTho's, Lidingö, Sweden). Ophthalmic ointment (Bepanthen, Bayer, Leverkusen, Germany) was applied to prevent corneal desiccation, and animals were monitored for the absence of pain reflexes. For analgesia, meloxicam (Metacam, Boehringer Ingelheim, Ingelheim am Rhein, Germany) was administered subcutaneously at a dose of 5 mg/kg prior to surgery. The scalp was disinfected with alternating applications of povidone-iodine solution (Betadine 10%, Egis Pharmaceuticals PLC, Budapest, Hungary) and 70% ethanol. Animals were then positioned in a stereotaxic frame (Kopf Model 962, David Kopf Instruments, Tujunga, CA, USA), and the skull was aligned using bregma and lambda as anatomical landmarks. A custom-made metallic headbar (Engineering Office M. Wohlwend GmbH, Sennwald, Switzerland) was secured with miniature skull screws and fixed with UV-curing glue (Vividye, USA) and dental acrylic (Paladur, Heraeus, Hanau, Germany) for long-term stability. After a 7-day postsurgical recovery period with daily monitoring, mice were handled for five days with a 10% sucrose reward and then habituated to head-fixation in the recording chamber over five days (10-30 min per day).

Pupil diameter recordings

To assess autonomic responses to hypercapnia, pupil size was recorded in head-fixed, non-locomoting mice during controlled exposure to increasing CO_2 concentrations. Experiments were conducted in the previously described CO_2 chamber under infrared illumination (wavelength: 780 nm - 1 mm) and constant low visible light (~10 lux). Gas was delivered at a constant flow rate of 9 L/min. CO_2 was increased stepwise to 10% and 20% with a recovery in synthetic air.

Mice were placed in the testing chamber and allowed to habituate for 5 min. The, baseline measurements were recorded for 5 min during an initial 5-min air exposure period (air1). CO_2 concentration was subsequently increased gradually from ambient levels to 10% CO_2 over approximately 8.5 min, followed by a 5-min stable 10% CO_2 exposure period. CO_2 concentration was then further increased from 10% to 20% over approximately 6.5 min. Although the protocol initially specified a 5-min stable 20% CO_2 exposure, pupil size reached a highly stable maximally dilated state with minimal temporal variation during 3 min and, thus, this phase was shortened to 3 min after the first recording in order to reduce overall exposure duration and potential stress to the animals. CO_2 delivery was then terminated, and chamber ventilation with synthetic air was maintained until CO_2 levels returned to baseline (0.3% CO_2). The washout period lasted approximately 10 min, after which a final 3-min air2 recording period (air2) was obtained before the end of the session.

Data analysis

Pupil size was recorded at 30 fps using a monochrome camera (DMK 27BUR0135) equipped with a TPL 0820 7MP objective lens (both from The Imaging Source, Bremen, Germany). Temporal synchronization with CO_2 levels which were recorded using a second identical camera was achieved using 20Hz hardware square-wave signal (5.0Vpp, +2.5V offset). Pupil area was extracted offline from recorded videos using the MEYE pupillometry platform, a convolutional neural network-based tool for automated pupil detection and tracking from video recordings[1]. The resulting pupil-size time series was exported and further processed in MATLAB using a customized multi-step filtering pipeline. First,

a median filter with a window length of 10 samples corresponding to 500ms at a sampling rate of 20Hz was applied to remove transient spikes and high-frequency noise. Subsequently, a Hampel filter with a window of ±10 samples (corresponding to 1s) was used to identify and correct statistical outliers while preserving the underlying signal dynamics. To correct for residual blink-related artifacts, samples falling below the 2nd percentile of the filtered pupil area distribution were identified as implausibly low values. These samples were treated as missing values and replaced by linear interpolation between neighboring valid samples. The resulting signal was then smoothed using a third-order Savitzky–Golay filter with a frame length of 21 samples (corresponding to 1.05s) to reduce remaining noise while preserving the temporal characteristics of the pupil response.

Following preprocessing, the pupil signal was downsampled from 20Hz to 5Hz using MATLAB's resample function. To reduce inter-animal variability in absolute signal amplitude (e.g., arising from slight differences in camera positioning), pupil size in pixels was normalized within each recording by expressing each sample as a percentage of the maximum pupil size observed in that recording. Specifically, each pupil-size value was divided by the recording-specific maximum pupil diameter and multiplied by 100, yielding a relative pupil-size measure expressed as a percentage of maximum pupil size.

Normalized pupil-size signals were retained for subsequent analyses. Stable time segments from each experimental phase including chamber habituation, air1, 10%CO_2, 20%CO_2, and air2, were truncated to a uniform length of 2495 frames corresponding to 124.75s. Mean pupil size was calculated for each segment and animal for statistical analysis.

c-Fos immunohistochemistry

c-Fos immunohistochemistry was performed according to our standard protocol[4].

Procedure

Two hours after the onset of the CO_2 challenge test, animals were deeply anesthetized and transcardially perfused with 0.9% saline followed by 4% paraformaldehyde in 0.2 M phosphate buffer

(PB) using a peristaltic pump (WPI Peristar Pro 4LS, World Precision Instruments, Sarasota, FL, USA). Brains were removed and postfixed at 4°C overnight. Brains were sectioned coronally at 40 µm on a vibratome (VT1000S, Leica Biosystems, Germany), and free-floating sections were matched by bregma level across experimental groups before being processed for c-Fos immunohistochemistry. Briefly, sections were incubated in a polyclonal rabbit anti-c-Fos primary antibody (1:1500, ab222699, Abcam, Waltham, MA, USA) for 72 h followed by a biotinylated goat anti-rabbit secondary antibody (1:500; Vector Laboratories, Burlingame, CA, USA). Signal amplification was performed using an avidin–biotin–horseradish peroxidase complex (Vectastain ABC Kit, Vector Laboratories, USA). c-Fos-positive cells were visualized using 3,3'-diaminobenzidine tetrahydrochloride (DAB; Sigma-Aldrich, Darmstadt, Germany) as chromogen.

Quantification of c-Fos-positive cells

The number of c-Fos-positive cells was quantified from images digitized with a scanner (LED Panoramic 250 Flash III scanner, 3DHISTECH, Budapest, Hungary) equipped with a 16-bit 4.2 MP camera at a magnification of 20× using ImageJ software (National Institutes of Health, Bethesda, Maryland, USA). A cell was considered as c-Fos-positive if the brown-black 3,3-diaminobenzidine-stained nucleus was unambiguously darker than the background staining, and this included all cells from low to high intensities of staining. c-Fos-positive cells were quantified within representative square regions of 0.0025-0.01 mm^2 placed into regions of interest according to the Mouse Brain in Stereotaxic Coordinates, fifth edition[5].

Functional network construction and analysis

Pearson's correlations were used for two complementary analyses: (i) associations between regional c-Fos expression and behavioural parameters were analysed across the complete dataset, including all experimental groups, and (ii) interregional co-activation of c-Fos expression was assessed separately

within the air control, 10% CO_2, and 20% CO_2 groups. For each group, Pearson's correlation coefficients and corresponding two-tailed p-values were calculated between all pairs of brain regions based on c-Fos expression levels. Significant correlations were defined as $p<0.05$ and used for exploratory network construction. No correction for multiple testing was applied to the correlation analyses because of the exploratory nature of the present study according to previous recommendations[6,7].

In the resulting undirected weighted networks, nodes represented individual brain regions and edges represented significant interregional c-Fos correlations. Both positive and negative correlations were retained to capture the full range of co-activation relationships, with positive correlations interpreted as coordinated c-Fos co-expression and negative correlations as inverse interregional relationships across animals within each group. Network visualization and graph-theoretical analyses were performed in Python using NetworkX (version 3.6.1). Layouts were generated using the spring layout algorithm, node size was scaled according to degree centrality, and edge width according to the absolute correlation coefficient. Positive and negative correlations were displayed in distinct colours.

Community structure was identified using the Louvain algorithm[8] implemented in the python-louvain package (version 0.16). This method detects communities of nodes that are more densely connected to each other than to nodes outside the community. The number of nodes, total number of edges, number of positive and negative edges, network density, degree centrality, top hub regions, and community composition were extracted and compared across experimental groups. Network density was defined as the ratio of observed edges to the maximum possible number of edges for the corresponding number of nodes.

To compare network topology across conditions, significant correlations were classified as shared, newly emerging, or lost between groups. For each CO_2 condition, new correlations were defined as significant correlations present in the CO_2 group but absent in the air control group, whereas lost correlations were defined as correlations present in air controls but absent in the respective CO_2 group. The same approach was used for the direct comparison between 10% and 20% CO_2 networks, with positive and negative correlations quantified separately. This comparative analysis allowed identification of concentration-dependent changes in interregional c-Fos co-activation patterns.

Key structural hubs within the network were identified by degree centrality calculated for all nodes within each designated group. To this end, degree centrality measures the proportion of direct connections a specific node holds relative to the total number of possible connections in the entire network. Centrality scores were indexed, sorted in descending order and then ranked based on these scores, and the top five highest-scoring nodes were extracted to identify the primary hub nodes responsible for local connectivity and localized information flow within the respective network topologies.

All these computational analyses were performed in Python 3 using pandas (version 2.2.2), NumPy (version 2.0.2), and SciPy (version 1.16.3) for data handling and numerical analyses, seaborn/matplotlib /version 0.13.2/3.10.0) for heatmap generation, and NetworkX (version 3.6.1) and python-louvain (version 0.16) for graph construction, network analysis, and community detection.

Data presentation and statistics

Data are presented as mean ± SEM. Statistically significant outliers were identified using Grubbs' test and excluded from further statistical analysis. After confirming normality using the Shapiro-Wilken test, behavioural data and c-Fos expression were analysed by one-way analysis of variance (ANOVA) followed by Tukey's multiple comparisons test or Welch's ANOVA followed by Dunnett's T3 multiple comparisons test. Correlations between behavioural measures and c-Fos expression, as well as correlations between c-Fos expression levels across brain regions, were assessed using Pearson correlation analyses. Effects were considered statistically significant at $p < 0.05$.

References

1 Mazziotti R, Carrara F, Viglione A, Lupori L, Lo Verde L, Benedetto A *et al.* MEYE: Web App for Translational and Real-Time Pupillometry. *eNeuro* 2021; **8**: ENEURO.0122-21.2021.

2 McMurray KMJ, Gray A, Horn P, Sah R. High Behavioral Sensitivity to Carbon Dioxide Associates with Enhanced Fear Memory and Altered Forebrain Neuronal Activation. *Neuroscience* 2020; **429**: 92–105.

3 Singewald GM, Rjabokon A, Singewald N, Ebner K. The Modulatory Role of the Lateral Septum on Neuroendocrine and Behavioral Stress Responses. *Neuropsychopharmacol* 2011; **36**: 793–804.

4 Muigg P, Scheiber S, Salchner P, Bunck M, Landgraf R, Singewald N. Differential Stress-Induced Neuronal Activation Patterns in Mouse Lines Selectively Bred for High, Normal or Low Anxiety. *PLoS ONE* 2009; **4**: e5346.

5 Paxinos G, Franklin KBJ. *Paxinos and Franklin's The Mouse Brain in Stereotaxic Coordinates*. 5th ed. Elsevier Science, 2019.

6 Kriegeskorte N, Simmons WK, Bellgowan PSF, Baker CI. Circular analysis in systems neuroscience: the dangers of double dipping. *Nat Neurosci* 2009; **12**: 535–540.

7 Eklund A, Nichols TE, Knutsson H. Cluster failure: Why fMRI inferences for spatial extent have inflated false-positive rates. *Proceedings of the National Academy of Sciences* 2016; **113**: 7900–7905.

8 Blondel VD, Guillaume J-L, Lambiotte R, Lefebvre E. Fast unfolding of communities in large networks. *J Stat Mech* 2008; **2008**: P10008.

Supplementary Table 1. Community composition of group-specific c-Fos co-activation networks

Community	Air	10% CO_2	20% CO_2
C0	BAR	CM	A24a +0.14
	CeM	DG	A24b +1.70, +0.50, +0.14
	DMPAG	DLPAG	A25 +1.70
	DP +1.70	DR	AID +1.77
	LC	M1 +0.35	DI +1.77
	LPBC	M2 +0.35	DP +1.70
	LPBI	LPAG	M1 +1.70, +0.14
	M2 +1.70, +0.50	MDM	M2 +1.70+0.14
	M1 +1.70, +0.50, +0.35	MDC	LSD
	LSD	PC	LSI
	Re	Po	MDM
	STL	Re	LDDM
		SolV	LPMR
		SolM	
		VLPAG	
C1	AIV +1.77	A24a +0.35	A24b +0.35
	AID +1.77	A24b +1.70	BAR
	BLA	BLA	CA1
	CeL	IMD	CA2
	CeC	LSI	CL
	CL	LSV	DLPAG
	CM	STLD	LDVL
	CA1	STLP	LC
	CA3	STLV	LPBI
	DI +1.77	STMA	LSV
	DR	STMV	M2 +0.35
	LaDL	PaLM	MDC
	LDDM	PaMM	MPB
	LDVL	Rh	MPBE
	LPLPAG	SolC	PC
	MDC	SolD	PCGS
	MDM,		
	MHb		
	MPB		
	MPBE		
	MR		
	PaMM		
	Po		
	Rh		
	SolV		
	VLPAG		

C2	A24a +0.14 A24b +0.14 DG DLPAG MDL PaMP	AID +1.77 AIV +1.77 Ang BAR CeL CeC LPBC LPBI LSD M2 +1.70, +0.50 M1 +1.70, +0.50, +0.14 MDLDI +1.77 MPB MPBE Slu	A24a +0.50 Ang DR LPBC Po STLP STLV PaLM SolC SolD SolM SolV
C3	A24a +1.70, +0.50, +0.35 A24b +1.70, +0.50, +0.35 A25 +1.70 Ang CA2 LSI LSV PaLM PC PV STLD STLV STMA STMV	A24a +1.70,+0.50, +0.14 A24b +0.50, +0.35, +0.14 A25 +1.70 M2 +0.14, CA1 CA2 CA3 CeM CL DMPAG DP +1.70 LaDL LC LDDM LDVL LHb LPMR MHb PaMP PaV PV	BLA CeM CM DG IMD LHb LPAG M1 +0.50, +0.35 M2 +0.50 MHb PaMP Rh VLPAG
C4	IMD LHb M1 +0.14 M2 +0.35, +0.14 PCGS SolM SolC SolD		A24a +0.35 CeL DMPAG PV STLD STMA Slu
C5			CA3 CeC LaDL MDL PaMM PaV Re

Brain regions were assigned to communities using Louvain community detection based on significant interregional Pearson correlations of c-Fos expression within each experimental group. Columns show the detected communities for air control, 10% CO_2, and 20% CO_2 conditions. Each entry lists the brain regions included in the respective community; rostrocaudal coordinates are indicated where applicable. The table illustrates CO_2 concentration-dependent changes in network organisation,

including the redistribution of cortical, limbic, thalamic, hypothalamic, brainstem, and periaqueductal grey regions across communities. *Abbreviations:* A24a: Cingulate cortex, area 24a or prelimbic cortex; A24b: Cingulate cortex, area 24b or cingulate cortex, area 1; A25: Cingulate cortex, area 25 or infralimbic cortex; AID, AIV: dorsal, ventral part of the agranular insular cortex; Ang: angular part of the thalamus; Bar: Barrington's nucleus; BLA: basolateral amygdala; CA1, CA2, CA3: hippocampal subfields; CeC, CeL, CeM: capsular, lateral, medial part of the central amygdala, CL, CM: centrolateral, centromedial part of the thalamus, DI: Dysgranular insular cortex; DLPAG, DMPAG: dorsolateral, dorsomedial part of the PAG; DP: Dorsal peduncular cortex; DRD, DRV: dorsal, ventral part of the Dorsal raphe; IMD: intermediodorsal part of the thalamus; LaDL: dorsolateral part of the lateral amygdala; LC: Locus coeruleus; LDDM, LDVL: dorsomedial, ventrolateral part of the laterodorsal thalamus, LPAG: lateral part of the PAG; LPBC, LPBI, LPMR: centrolateral, internolateral, mediorostral part of the lateral parabrachial nucleus; LSD, LSI, LSV: dorsal, intermediate, ventral part of the lateral septum, M1, M2: primary, secondary motor cortex; MDC, MDL, MDM: central, lateral, medial part of the mediodorsal thalamus; MPB, MPBE: Medial parabrachial nucleus including external part; PAG: periaqueductal grey; PALM, PaMM, PaMP PaV: lateral magnocellular, medial magnocellular, medial parvicellular part, ventral part of the paraventricular hypothalamus, PC: paracentral part of the thalamus; PCGS: Paracochlear glial substance; Po: posterior part of the thalamic group; PV: Paraventricular thalamus; Re: Reuniens thalamus; Rh: Rhomboid thalamus; SolC, SolDL, SolIM, SolVL: commissural, dorsolateral, medial ventrolateral part of the solitary nucleus; STLD, STLP, STLV, STMA, STMV: dorsolateral, posterolateral, ventrolateral, anteromedial medioventral divisions of the Bed nucleus of stria terminalis; VLPAG: ventrolateral part of the PAG.

Supplementary Table 2. Top five hub nodes by degree centrality in the c-Fos co-activation network for each experimental condition

Rank	air		20% CO2		10% CO2	
	hub	**centrality**	**hub**	**centrality**	**hub**	**centrality**
1	MDC	0.270	M1 +0.14	0.365	LDDM	0.250
2	DI +1.77	0.203	CA3	0.270	M1 +0.35	0.222
3	Po	0.203	LPAG	0.270	CM	0.222
4	AIV +1.77	0.189	M1 +0.35	0.256	M2 +0.35	0.208
5	CA1	0.189	MDM	0.256	A24b +0.14	0.208

Degree centrality values reflect the number of significant co-activation links per node, normalized to the network. Numbers behind brain area indicate the approximate rostro-caudal level relative to bregma according to the brain atlas of Paxinos and Watson[5]. Abbreviations: A24b: Cingulate cortex, area 24b or cingulate cortex, area 1; AIV: ventral part of the agranular insula; CA1, CA3: CA1, CA2, CA3: hippocampal subfields; CM: centromedial part of the thalamus; DI: dysgranular insula; LDDM: dorsomedial, ventrolateral part of the laterodorsal thalamus; LPAG: lateral periaqueductal grey; M1: primary motor cortex; M2: secondary motor cortex; MDC: central part of the mediodorsal thalamus; MDM: medial part of the mediodorsal thalamus; Po: posterior part of the thalamic group.

Supplementary Figure 1

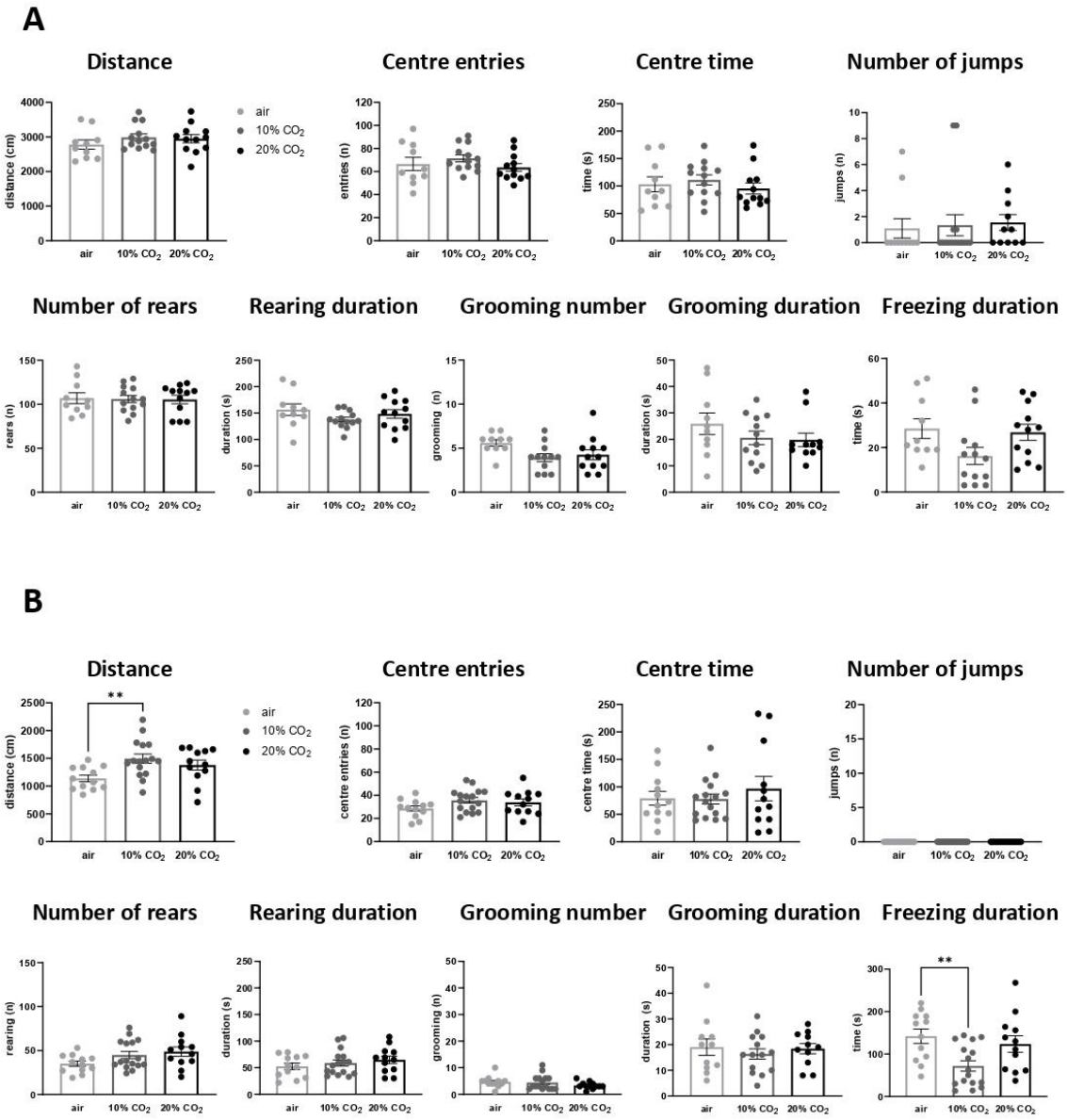

Supplementary Figure 1 | Behavioural responses during habituation to the experimental chamber and synthetic air exposure. (A) Mice were placed in the chamber without gas manipulation for 10 min (Day 1). Behavioural parameters, including distance travelled, centre entries, centre time, number of jumps, number of rears, rearing duration, grooming number, grooming duration, and freezing duration, were quantified. No significant differences were observed between groups later assigned to air, 10% CO_2, or 20% CO_2. **(B)** Mice were exposed to synthetic air (<0.1% CO_2) for 10 min. Behavioural parameters, including distance travelled, centre entries, centre time, number of jumps, number of rears, rearing duration, grooming number, grooming duration, and freezing duration, were quantified. Distance travelled was increased in mice later assigned to the 10% CO_2 group, and freezing duration was reduced. No other behavioural parameters differed between groups. Data are presented as mean ± SEM with individual data points (n = 12–16). ***P* < 0.05, analysed by one-way ANOVA followed by Tukey's post-hoc test or Welch's ANOVA test followed by Dunnett's T3 post-hoc test, where appropriate.

Supplementary Figure 2

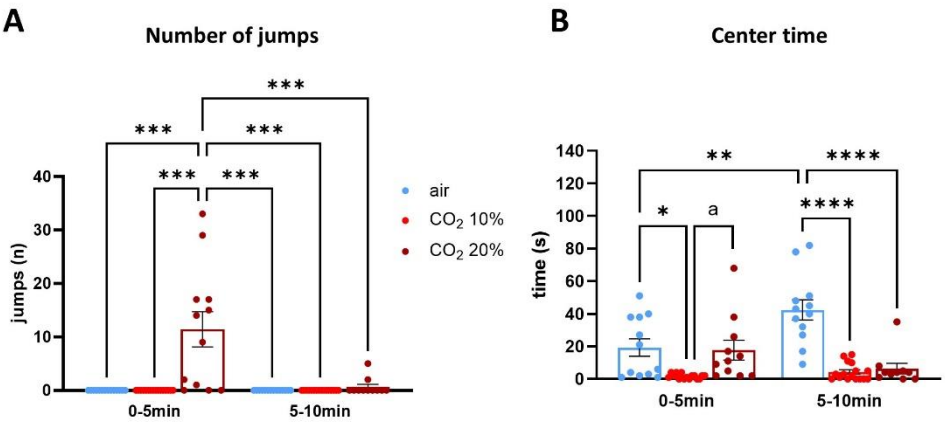

Supplementary Figure 2 | CO_2-induced jumping was strongest in the first half of exposure. (A) Number of jumps counted in the first and second 5 min bins of the 10 min CO_2 exposure. Jumping was greater in the first 5 min and declined during the second 5 min. **(B)** In line with the temporal pattern of jumping behaviour, time spent in the centre of the testing arena did not differ during the first half of the testing period, but was reduced during the second half as compared with air control. Data are presented as mean ± SEM with individual data points (n = 11–16). [a] P <0.08, ** P <0.01, *** P <0.001, analysed by two-way ANOVA followed by Tukey's post-hoc test.